SCIENCE CHINA Materials ARTICLES

mater.scichina.com link.springer.com

Published online 26 December 2018 | https://doi.org/10.1007/s40843-018-9381-1

Sci China Mater 2019, 62(6): 797–802

Enhancing back interfacial contact by *in-situ* prepared MoO_3 thin layer for $Cu_2ZnSnS_xSe_{4-x}$ solar cells

Xue Min[1,3], Linbao Guo[1,3], Qing Yu[1,3], Biwen Duan[1,3], Jiangjian Shi[1], Huijue Wu[1], Yanhong Luo[1,3,4], Dongmei Li[1,3,4*] and Qingbo Meng[1,2,4*]

ABSTRACT ***In-situ* prepared MoO_3 thin layer has been introduced to suppress the formation of too thick $Mo(S,Se)_2$ layer in $Cu_2ZnSnS_xSe_{4-x}$ (CZTSSe) solar cells. This MoO_3 layer effectively improves the back interfacial contact between CZTSSe absorber layer and Mo substrate without poisoning the carrier transport. Up to 10.58% power conversion efficiency has been achieved.**

Keywords: $Cu_2ZnSnS_xSe_{4-x}$ solar cells, MoO_3 blocking layer, *in-situ* preparation, back interfacial contact, carrier transport

INTRODUCTION

Kesterite $Cu_2ZnSnS_xSe_{4-x}$ (CZTSSe) is a kind of new generation solar cell absorber material, which has similar crystal structure to chalcopyrite $Cu(In,Ga)Se_2$ (CIGS). Recently, CZTSSe has received much attention due to its high absorption coefficient (higher than 10^4 cm^{-1}), adjustable bandgap (1.0–1.5 eV) and well matching to solar spectrum [1,2]. Typically, elements in this material are abundant in earth and environmentally friendly, which is suitable for high-efficiency, low-cost and stable solar cells [3–6].

CZTSSe solar cells have similar structure with CIGS solar cells, with molybdenum (Mo) metal back electrode. A high temperature selenization in the fabrication of CZTSSe absorber layer results in a $Mo(S,Se)_2$ layer between CZTSSe absorber layer and Mo electrode. Appropriate thickness of $Mo(S,Se)_2$ can form ohmic contact with CZTSSe to promote an adhesion between the absorber layer and the Mo substrate and thus be favorable for the cell performance. However, too thick $Mo(S,Se)_2$ layer would raise a series resistance (R_S) in the solar cell to impede the carrier transport [7,8]. In addition, CZTSSe absorber layer reacts with Mo substrate at high temperatures, leading to the phase decomposition of CZTSSe [9]. Therefore, the modification of the back contact interface is essential to improving the performance of solar cells.

Much attention has been paid to improving the back contact interface. Zhang *et al.* [10] prepared a temporary dense alloy layer for CZTSe solar cells by sputtering deposition, which effectively suppressed the formation of $MoSe_2$. Guha *et al.* [11] introduced a TiN diffusion barrier between CZTSe and Mo to suppress the formation of $MoSe_2$, which gave the CZTSe solar cell with the efficiency of 8.9% and long photon-generated carrier lifetimes. Liu *et al.* [12] inserted a thin TiB_2 intermediate layer at CZTS/Mo interface, which eliminated the MoS_2 layer and endowed the CZTS absorber with large grains.

In this work, we adopt *in-situ* pre-annealing method to treat the Mo substrate for MoO_3 thin layers to improve the interfacial contact between CZTSSe absorber layer and Mo substrate for CZTSSe solar cells. The influence of different annealing temperatures on the MoO_3 layer thickness and the cell performance has been explored. It is found that annealed substrates can suppress the formation of $Mo(S,Se)_2$. However, too thick MoO_3 leads to high R_S. Optimal pre-annealing temperature of 350°C can afford a suitable MoO_3 thickness to effectively reduce the thickness of $Mo(S,Se)_2$ without impeding the carrier

[1] Key Laboratory for Renewable Energy (CAS), Beijing Key Laboratory for New Energy Materials and Devices, Beijing National Laboratory for Condense Matter Physics, Institute of Physics, Chinese Academy of Sciences (CAS), Beijing 100190, China
[2] Center of Materials Science and Optoelectronics Engineering, University of Chinese Academy of Sciences, Beijing 100049, China
[3] School of Physical Sciences, University of Chinese Academy of Sciences, Beijing 100049, China
[4] Songshan Lake Materials Laboratory, Dongguan 523808, China
* Corresponding authors (emails: qbmeng@iphy.ac.cn (Meng Q); dmli@iphy.ac.cn (Li D))

transport. The efficiency up to 10.58% has been achieved. This method is simple and cost-effective without introducing other barrier material and may have potential large-scale application in the future.

EXPERIMENTAL SECTION

Ethanolamine ($HOCH_2CH_2NH_2$, 99.0%), thioglycolic acid ($HSCH_2COOH$, 98%) and 2-methoxyethanol ($HOCH_2CH_2OCH_3$, 99.5%) were purchased from Aladdin. CuO (99.99%, ZhongNuo), ZnO (99.99%, Sigma-Aldrich) and SnO (99.9%, Aladdin) were used as metal sources. Se particles (99.999%) were purchased from ZhongNuo Advanced Material (Beijing) Technology Co., Ltd. All the chemicals were directly used as received without further purification. Mo-sputtered soda lime glass (SLG) substrates were bought from Jinan Lister Electronic Equipment Department.

Mo electrodes of ~800 nm thickness on the SLG were cleaned with ethanol before pre-annealing. Then, the clean Mo substrate was annealed in a rapid thermal processing (RTP) furnace under the synthetic air flow. The gas flow rate was maintained at 60 sccm and the pressure in the chamber was kept at a normal pressure. Here, three annealing temperatures (350, 400 and 450°C) were adopted, and the annealing time was 15 min. And the products were labeled as 350-Mo, 400-Mo and 450-Mo, respectively.

The CZTSSe absorber was prepared as our previous work [12,13]. Briefly, 0.1400 g CuO, 0.0977 g ZnO and 0.1347 g SnO were dissolved into a mixed solvent composed of 4 mL 2-methoxyethanol, 2 mL ethanolamine and 1.2 mL thioglycolic acid. A clear yellow precursor solution was obtained after 120 min stirring. CZTS precursor films were prepared by spin-coating the precursor solution on the Mo or annealed Mo substrates at 3,000 rpm and followed by an annealing process at 330°C on a hot plate for 2 min in a N_2-filled glovebox. The spin-coating step was repeated five times to give a desired thickness. CZTSSe absorber was obtained by selenization in the RTP furnace. Especially, the CZTS precursor film and 1.0 g Se particles were put into a quasi-closed graphite box, and then annealed at 540°C for 15 min under N_2 flow (10^5 Pa).

CZTSSe solar cells were fabricated with the structure of SLG/Mo/CZTSSe/CdS/ZnO/ITO/Ag. A 50 nm-thickness CdS buffer layer was deposited onto the CZTSSe absorber by the chemical bath deposition (CBD), followed by the radio frequency (RF) sputtering of 50 nm ZnO and 250 nm ITO as the window layer. Finally, a Ag grid was deposited by thermal evaporation at 10^{-7} Torr.

X-ray diffraction (XRD) patterns of as-prepared samples were collected by an X-ray diffractometer with Cu Kα line as the radiation source (Empyrean, PANaltcal). The morphologies of as-prepared films and devices were observed by a scanning electron microscope (S4800-SEM, Hitachi). The square resistances of the substrates were measured by a four-probe resistivity tester (RTS-9, Probes Tech). Some MoO_3 on annealed Mo substrates was etched with concentrated ammonia, and then its thickness was measured by a profiler (P-6, KLA Tech). Current density-voltage (J–V) characteristics of the cells were collected on Keithley 2400 SourceMeter under AM1.5G illumination (1,000 W m^{-2}) from Zolix SS150A. The light intensity of the solar simulator was calibrated by a standard monocrystalline silicon reference solar cell. The active area and total area of the cell are 0.1800 and 0.2025 cm^2, respectively.

RESULTS AND DISCUSSION

Untreated Mo substrates are argenteous under white light LED illumination. After being annealed in the air, the surface color of Mo substrates changes a lot. The Mo substrate treated at 350°C (350-Mo) is isabelline with metallic luster, blue with metallic luster for 400-Mo samples, and gray without metallic luster for 450-Mo samples. It is known that Mo reacts with oxygen at high temperatures to produce molybdenum oxide (MoO_x) where x is dependent on the oxygen amount in the reaction. At low oxygen content, MoO_2 is the main product [13], while MoO_3 is obtained under sufficient oxygen [14]. MoO_2 do not react with acids or bases, whereas MoO_3 is easily soluble in acids and bases. Here, we dribbled concentrated ammonia on the 450-Mo substrate, and found that the gray layer on the substrate surface rapidly dissolved to give argenteous Mo layer. Similar phenomena are also observed for 350-Mo and 400-Mo samples, suggesting that MoO_3 is formed on the Mo surface after being annealed. Top-view SEM images of Mo substrates before and after annealing (Fig. 1a–d) show the wedged grains at the surface of the untreated Mo substrate, while the annealed Mo substrate presents elliptical grains. As the annealing temperature increases, the grain sizes increase from tens of nanometers to hundreds of nanometers. In Fig. 1e, Mo thickness of the untreated substrate is about 830 nm. An extra MoO_3 thin layer is found on the surface of 350-Mo and 400-Mo substrates with similar Mo thickness. MoO_3 thickness on the annealed Mo substrates is determined by a profiler. As shown in Table 1, the MoO_3 thickness increases with increasing annealing temperatures from 350 to 450°C,

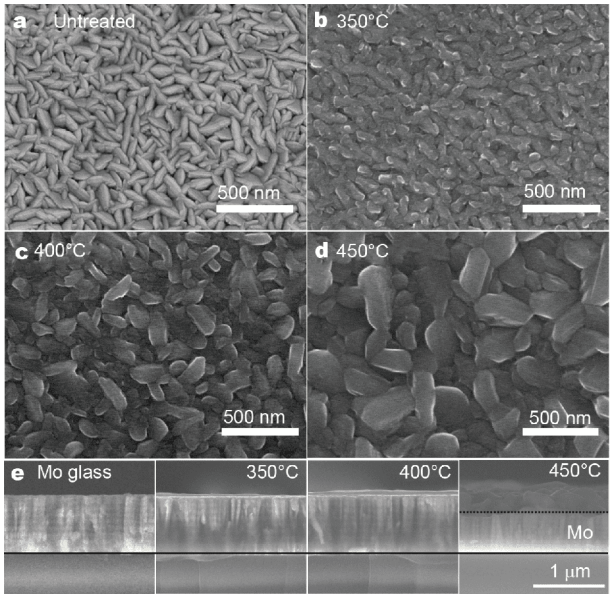

Figure 1 Top-view SEM images of Mo substrates annealed at different temperatures for 15 min: (a) untreated Mo substrate; (b) 350-Mo; (c) 400-Mo; (d) 450-Mo; (e) cross-sectional SEM images of the four samples (scale bar: 1 μm).

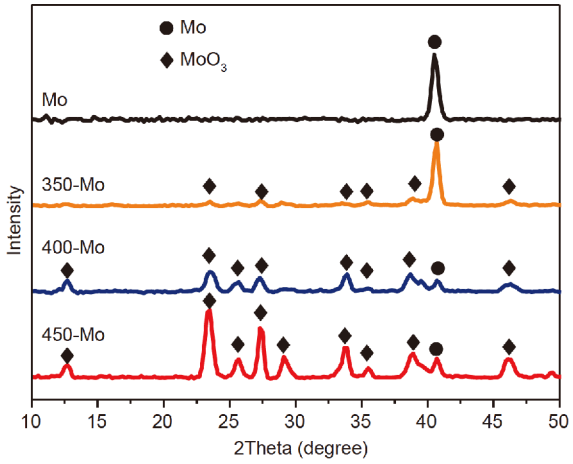

Figure 2 Grazing incidence XRD patterns of different substrates.

Table 1 Electrical properties of Mo substrates and the MoO_3 film thickness

Substrates	Square resistance (mΩ sq^{-1})	Thickness (nm)
Mo	327	/
350-Mo	359	52.5
400-Mo	474	111.7
450-Mo	610	350

suggesting that MoO_3 thickness is controlled by changing annealing temperatures and fixing annealing time. However, at 450°C, the MoO_3 thickness rises to 350 nm, five times thicker than that of 350-Mo sample, while its Mo thickness reduces to 560 nm.

The surface crystal structure of the annealed Mo substrates was investigated by grazing incidence XRD. The grazing incidence uses an angle of 0.5° to detect the information of the substrate surface. In Fig. 2, only one peak at 40.7° is found in the untreated Mo substrate. For the annealed Mo substrate, the peaks at 12.6°, 23.5°, 25.7°, 27.4°, 29.1°, 33.8°, 35.5°, 38.9° and 46.1° assigned to MoO_3 suggest that MoO_3 is indeed formed on the surface of the Mo substrate after annealing [15]. Besides, increasing annealing temperature leads to the decreasing half-width ratio of MoO_3 peaks gradually, indicating better crystallinity of MoO_3 and larger crystal sizes on the surface of the Mo substrate.

Electric conductivity of Mo substrate as bottom electrode is critical to the CZTSSe solar cell performance. Introduction of MoO_3 on the Mo surface can effectively suppress the formation of $Mo(S,Se)_2$, although MoO_3 has poor electric conductivity. Therefore, a suitable MoO_3 thickness is important for high-efficiency devices because it strongly affects the carrier transport [16]. Table 1 lists square resistances of the as-prepared substrates. No obvious difference in the square resistance (below 360 mΩ sq^{-1}) is found between the 350-Mo and untreated Mo substrates. However, for 400-Mo and 450-Mo samples, their square resistances are significantly higher than that of the untreated Mo substrate.

CZTSSe absorber layers were spin-coated on the four substrates [17,18]. No obvious difference is observed in the morphologies of the precursor film and the CZTSSe crystal film on different substrates. According to XRD patterns of CZTSSe absorber layer on different substrates in Fig. 3a, there is no significant difference in the (112) peak of CZTSSe phase and the crystallinity of CZTSSe films on the annealed Mo substrates. For the untreated Mo substrate, XRD pattern in the range of 30–34° corresponding to $Mo(S,Se)_2$ is found. However, it is not found for annealed Mo substrate samples (Fig. 3b). Obviously, the MoO_3 layer derived from high temperature pre-annealing process effectively blocks the formation of $Mo(S,Se)_2$ [19].

Cross-sectional SEM images of CZTSSe solar cells on the different Mo substrates are given in Fig. 4. The morphologies of CZTSSe absorber layers on different substrates are similar, which are divided into two layers, the upper large-crystal layer and the bottom small-grain layer. A $Mo(S,Se)_2$ layer in the untreated Mo substrate has

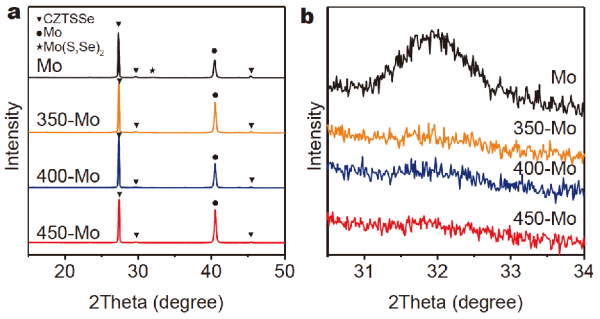

Figure 3 (a) XRD patterns of CZTSSe samples on different Mo substrates; (b) zoomed XRD patterns in the range of 30–34°.

the thickness of ~535 nm (Fig. 4a). The Mo thickness of 350-Mo and 400-Mo samples is ~830 nm, close to untreated Mo glass (Fig. 4e). And no obvious MoO_3 layer can be found, suggesting that the as-prepared MoO_3 thin layer converts into $Mo(S,Se)_2$. For 450-Mo substrate, however, the thickness of the Mo layer does not obviously change before and after the selenization, and no obvious $Mo(S,Se)_2$ or MoO_3 thin layers are found either, as shown in Fig. 1e and 4e. A thick small-grain layer between the CZTSSe crystal layer and the Mo substrate suggests that there may be some $Mo(S,Se)_2$ with a small amount of unreacted MoO_3 at the bottom of the CZTSSe fine grain layer, because too thick MoO_3 layer is not completely converted to $Mo(S,Se)_2$ in the selenization process. However, it is too hard to accurately estimate the $Mo(S,Se)_2$ and MoO_3 thickness. This phenomenon further confirms that this *in-situ* prepared MoO_3 layer indeed acts as the interfacial blocking layer to impede the formation of $Mo(S,Se)_2$.

CZTSSe solar cells were further assembled with the structure of SLG/Mo/CZTSSe/CdS/ZnO/ITO/Ag to investigate the effect of different Mo substrates on the cell performance. As shown in Fig. 5a and Table 2, the 350-Mo substrate shows the champion efficiency of 10.58% with a short-circuit current density (J_{SC}) of 36.09 mA cm^{-2}, an open circuit voltage (V_{OC}) of 447.75 mV and a fill factor (FF) of 65.4%, while the device efficiency based on the total area is 9.40%. Besides, the average efficiency of the devices based on 350-Mo substrates is 6.3% higher than that of the control group, while the average photoelectric conversion efficiency (PCE) of CZTSSe solar cells on 400-Mo and 450-Mo substrates decreases. And external quantum efficiency (EQE) spectra of CZTSSe solar cells based on 350-Mo and untreated Mo substrates are also shown in the inset of Fig. 5a. PCEs, J_{SC}, V_{OC} and FF of six solar cells on each substrate (Fig. 5b–e) statistically show that the different

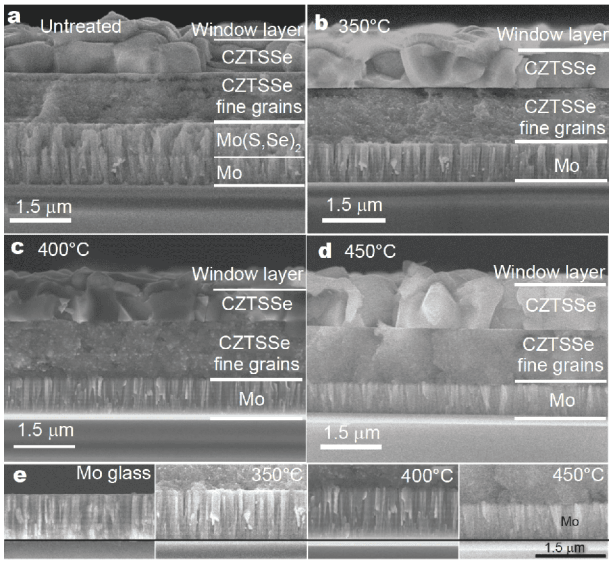

Figure 4 Cross-sectional SEM images of CZTSSe solar cells on Mo substrates annealed at different temperatures for 15 min: (a) untreated Mo sample; (b) 350-Mo; (c) 400-Mo; (d) 450-Mo; (e) enlarged images of Mo layers of Mo glass, 350-Mo (b), 400-Mo (c) and 450-Mo (d).

cell performance mainly results from the FF because high R_S leads to low FF. In Fig. 5f, the average R_S of the devices on 350-Mo substrates is about 1.92 Ω, lower than 2.38 Ω of untreated Mo samples, in accordance with the cell performance. This also verifies that MoO_3 on the 350-Mo substrate effectively suppresses the formation of $Mo(S,Se)_2$ without poisoning the carrier transport and collection. However, compared with R_S of the untreated and 350-Mo substrates, R_S of the solar cells on 400-Mo and 450-Mo substrates further increase and thus result in poor FF of the devices. In addition, the slight increase of V_{OC} of 350-Mo sample suggests that the MoO_3 with a suitable thickness also reduces the interface recombination and improves V_{OC} [20]. However, too thick MoO_3 layer on the 400-Mo and 450-Mo substrates hinders carrier transport and collection, and even becomes interfacial recombination centers, thus reducing V_{OC}. In terms of the overall performance, the optimal pre-annealing temperature is 350°C.

CONCLUSIONS

A thin MoO_3 layer is introduced between Mo substrate and CZTSSe absorber film by *in-situ* pre-annealing the Mo substrate in air to suppress the formation of too thick $Mo(S,Se)_2$ layer during high-temperature selenization. With the increase of treatment temperature, the MoO_3 grains and the film thickness gradually increase. At optimal annealing temperature of 350°C, the CZTSSe thin

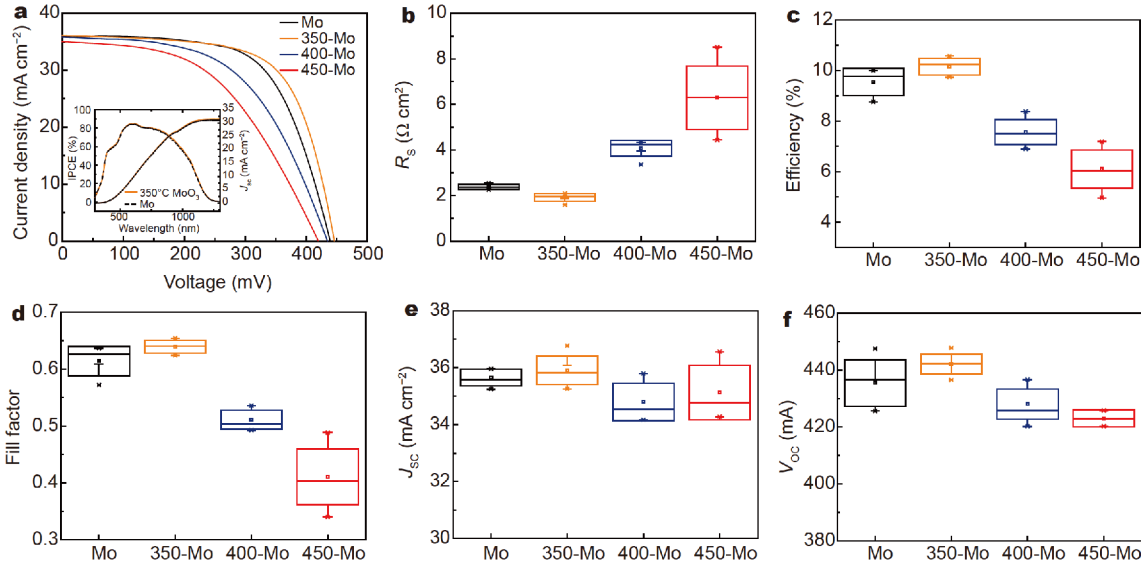

Figure 5 (a) *J*–*V* curves of CZTSSe solar cells on different substrates. Inset of Fig. 5a: EQE spectra of CZTSSe solar cells based on 350-Mo and untreated Mo substrates. The statistical box charts of solar cells: (b) PCE, (c) J_{SC}, (d) V_{OC}, (e) FF and (f) R_S.

Table 2 Photovoltaic performance characteristics of best and average (in parentheses) on different substrates

Samples	PCE (%)	V_{OC} (mV)	J_{SC} (mA cm^{-2})	FF (%)	R_S (Ω cm^2)
Mo	10.03 (9.55)	436.54 (435.45)	35.96 (35.66)	63.9 (61.4)	2.31 (2.38)
350-Mo	10.58 (10.15)	447.75 (442.11)	36.09 (35.91)	65.4 (63.9)	1.60 (1.92)
400-Mo	8.38 (7.62)	436.39 (428.05)	35.80 (34.81)	53.6 (51.1)	3.36 (4.07)
450-Mo	7.19 (6.10)	420.24 (422.99)	34.99 (35.13)	48.8 (41.1)	4.43 (6.29)

film solar cell presents the efficiency of 10.58%. The MoO_3 layer with appropriate thickness not only effectively suppresses the formation of $Mo(S,Se)_2$, but also enhances the back interfacial contact without impeding the carrier transport and collection.

Received 20 October 2018; accepted 12 December 2018; published online 26 December 2018

1 Zhou H, Hsu WC, Duan HS, *et al.* CZTS nanocrystals: a promising approach for next generation thin film photovoltaics. Energy Environ Sci, 2013, 6: 2822–2838
2 Polizzotti A, Repins IL, Noufi R, *et al.* The state and future prospects of kesterite photovoltaics. Energy Environ Sci, 2013, 6: 3171–3182
3 Chen S, Walsh A, Gong XG, *et al.* Classification of lattice defects in the kesterite Cu_2ZnSnS_4 and $Cu_2ZnSnSe_4$ earth-abundant solar cell absorbers. Adv Mater, 2013, 25: 1522–1539
4 Kumar M, Dubey A, Adhikari N, *et al.* Strategic review of secondary phases, defects and defect-complexes in kesterite CZTS–Se solar cells. Energy Environ Sci, 2015, 8: 3134–3159
5 Li J, Wang D, Li X, *et al.* Cation substitution in earth-abundant kesterite photovoltaic materials. Adv Sci, 2018, 5: 1700744
6 Yan C, Huang J, Sun K, *et al.* Cu_2ZnSnS_4 solar cells with over 10% power conversion efficiency enabled by heterojunction heat treatment. Nat Energy, 2018, 3: 764–772
7 Shin B, Bojarczuk NA, Guha S. On the kinetics of $MoSe_2$ interfacial layer formation in chalcogen-based thin film solar cells with a molybdenum back contact. Appl Phys Lett, 2013, 102: 091907
8 Yang KJ, Sim JH, Jeon B, *et al.* Effects of Na and MoS_2 on Cu_2ZnSnS_4 thin-film solar cell. Prog Photovolt-Res Appl, 2015, 23: 862–873
9 Scragg JJ, Wätjen JT, Edoff M, *et al.* A detrimental reaction at the molybdenum back contact in $Cu_2ZnSn(S,Se)_4$ thin-film solar cells. J Am Chem Soc, 2012, 134: 19330–19333
10 Li J, Zhang Y, Zhao W, *et al.* A temporary barrier effect of the alloy layer during selenization: tailoring the thickness of $MoSe_2$ for efficient $Cu_2ZnSnSe_4$ solar cells. Adv Energy Mater, 2015, 5: 1402178
11 Shin B, Zhu Y, Bojarczuk NA, *et al.* Control of an interfacial $MoSe_2$ layer in $Cu_2ZnSnSe_4$ thin film solar cells: 8.9% power conversion efficiency with a TiN diffusion barrier. Appl Phys Lett, 2012, 101: 053903
12 Liu F, Sun K, Li W, *et al.* Enhancing the Cu_2ZnSnS_4 solar cell efficiency by back contact modification: Inserting a thin TiB_2 intermediate layer at Cu_2ZnSnS_4/Mo interface. Appl Phys Lett, 2014, 104: 051105
13 Li W, Han X, Zhao Y, *et al.* Pre-annealing induced oxide barrier to suppress the over-selenization of Mo contact. J Mater Sci-Mater Electron, 2016, 27: 11188–11191
14 Chernova NA, Roppolo M, Dillon AC, *et al.* Layered vanadium and molybdenum oxides: batteries and electrochromics. J Mater Chem, 2009, 19: 2526–2552

15 Ding QP, Huang HB, Duan JH, *et al.* Molybdenum trioxide nanostructures prepared by thermal oxidization of molybdenum. J Cryst Growth, 2006, 294: 304–308
16 Kröger M, Hamwi S, Meyer J, *et al.* P-type doping of organic wide band gap materials by transition metal oxides: a case-study on molybdenum trioxide. Org Electron, 2009, 10: 932–938
17 Tian Q, Wang G, Zhao W, *et al.* Versatile and low-toxic solution approach to binary, ternary, and quaternary metal sulfide thin films and its application in $Cu_2ZnSn(S,Se)_4$ solar cells. Chem Mater, 2014, 26: 3098–3103
18 Min X, Shi J, Guo L, *et al.* Regulation of Zn/Sn ratio in kesterite absorbers to boost 10% efficiency of $Cu_2ZnSn(S,Se)_4$ solar cells. Chin Phys B, 2018, 27: 016402
19 Haass SG, Diethelm M, Werner M, *et al.* 11.2% Efficient solution processed kesterite solar cell with a low voltage deficit. Adv Energy Mater, 2015, 5: 1500712
20 Shin D, Saparov B, Mitzi DB. Defect engineering in multinary earth-abundant chalcogenide photovoltaic materials. Adv Energy Mater, 2017, 7: 1602366

Acknowledgements This work was financially supported by the National Natural Science Foundation of China (91733301, 51761145042, 51627803, 21501183, 51402348, 11474333, 91433205 and 51421002), the Knowledge Innovation Program and the Strategic Priority Research Program (Grant XDB 12010400) of the Chinese Academy of Sciences.

Author contributions Meng Q supervised the whole project. Li D proposed the preparation of materials and participated in the discussion. Min X, Guo L and Yu Q carried out the experiments for device fabrication, optimization and characterization. Duan B performed the HR-SEM measurement. Shi J, Wu H and Luo Y contributed to the data analysis and interpretation for the results.

Conflict of interest The authors declare no conflict of interest.

Xue Min received her bachelor degree in the School of Optical and Electronic Information, Huazhong University of Science and Technology in 2015, and received her master degree in the Institute of Physics (IOP), Chinese Academy of Sciences (CAS) in 2018. Her work mainly focused on developing highly efficient $Cu_2ZnSnS_xSe_{4-x}$ solar cells and related materials.

Dongmei Li is a full professor at IOP, CAS. She received her PhD from Jilin University in 1999. In 2000, she was a postdoctoral fellow in Nihon University. From 2001 to 2003, she was a research associate in Cardiff University, UK. From 2003 to 2005, she worked in the College of Chemistry, Jilin University. Since 2005, she has been working in the IOP. Her current research interest focuses on solar energy materials & devices, including new generation solar cells and photocatalytic materials. She has published over 170 papers, which were cited over 7,700 times (h-index 44), applied over 50 patents in which over 30 patents were authorized.

Qingbo Meng is currently a full professor at the IOP, CAS, director of Center for Clean Energy, IOP. He received his PhD degree in 1997 from Changchun Institute of Applied Chemistry, CAS. From 1997 to 1999, he was a postdoctoral fellow in the IOP. From 1999 to 2002, he was a STA Fellow (Science and Technology Agency of Japan) and Researcher of the University of Tokyo and KAST in Japan. He was selected as "Distinguished Young Scholars" from NSFC in 2007 and the project leader of the Fund for Creative Research Groups of China in 2014. He was awarded to "the Special Allowance of the State Council" in 2010 and "The President of the Tokyo University Science Award" in 2011. His current research interest focuses on solar energy materials & devices, including new generation thin film solar cells (such as perovskite solar cells, kesterite solar cells, quantum dot solar cells) and photocatalytic materials. He has published over 220 papers, which were cited over 8,600 times (h-index 55). He has applied over 80 patents, and over 50 patents were authorized.

原位制备MoO_3薄膜提高铜锌锡硫硒太阳能电池背界面接触性能

闵雪[1,3], 郭林宝[1,3], 于晴[1,3], 段碧雯[1,3], 石将建[1], 吴会觉[1], 罗艳红[1,3,4], 李冬梅[1,3,4*], 孟庆波[1,2,4*]

摘要 在空气中对钼基底进行退火处理, 在钼表面形成MoO_3薄层. 该MoO_3薄膜能有效抑制过厚$Mo(S,Se)_2$的形成. 研究发现, MoO_3厚度随着温度的升高而增大, 其中350°C形成的MoO_3厚度最为合适, 既能够有效降低$Mo(S,Se)_2$的厚度, 又不影响吸收层和钼电极接触, 器件最高效率达到10.58%. 这种方法不会引入其他杂质元素, 操作简单方便.

